Tandem Reflectron Time-of-Flight Mass Spectrometer Utilizing Photodissociation

ARTICLE *in* ANALYTICAL CHEMISTRY · DECEMBER 1995

Impact Factor: 5.64 · DOI: 10.1021/ac00117a021 · Source: PubMed

5 AUTHORS, INCLUDING:

Douglas J. Beussman
St. Olaf College
19 PUBLICATIONS **309** CITATIONS
SEE PROFILE

Mary Seeterlin
MDCH Michigan Department of Community H…
8 PUBLICATIONS **172** CITATIONS
SEE PROFILE

Chris Enke
University of New Mexico
198 PUBLICATIONS **4,630** CITATIONS
SEE PROFILE

Anal. Chem. **1995**, *67*, 3952–3957

Tandem Reflectron Time-of-Flight Mass Spectrometer Utilizing Photodissociation

Douglas J. Beussman, Paul R. Vlasak, Richard D. McLane,† Mary A. Seeterlin, and Christie G. Enke*

Department of Chemistry, Michigan State University, East Lansing, Michigan 48824

A tandem time-of-flight (TOF) mass spectrometer has been designed to obtain complete MS/MS spectra from compounds eluting from a gas chromatograph. This application requires high spectral generation rate, unit mass resolution for both precursor selection and product spectra, and efficient ion utilization. These objectives are achieved by reflectron TOF mass separation in both stages and laser photoinduced dissociation as the ion fragmentation method. Careful timing of the laser pulse relative to ion extraction allows ions of a single *m/z* value up to *m/z* 1000 to be photodissociated while ions with adjacent *m/z* values are essentially unaffected. The convergent foci of the ion packet and laser pulse results in ion fragmentation efficiencies as high as 79%. An ion gate prevents the nonselected precursor ions from convoluting the product spectra. Product spectra can be generated at the maximum laser repetition rate (currently 200 Hz). To achieve unit mass resolution for all product *m/z* values simultaneously, a novel reflectron was designed for the second TOF stage.

Tandem mass spectrometers have the capability of providing substantial improvements over single-stage mass spectrometers in both chemical selectivity and the amount of structural information obtained about an analyte. The complete tandem mass spectrometry (MS/MS) characterization of an analyte requires obtaining the product mass spectrum for each of the *m/z* values of interest in the primary mass spectrum. One of the most severely felt limitations is the amount of MS/MS data that can be collected on a compound introduced to the mass spectrometer after chromatographic separation, due to the requirement that the analyte partial pressure remain relatively constant in the source during the analysis time. For this application, it is desirable to be able to collect 100 or more product spectra per second. The high sensitivity desired for such an application also requires that at least the second mass analysis be performed by array detection rather than by scanning a mass filter. The existing true array detection mass spectrometric techniques include magnetic sector with spatial array detection and Fourier transform mass spectrometry, while time-of-flight (TOF) with time array detection and the ion trap are batch array detection techniques.

In this paper, the design and performance of an instrument intended to obtain MS/MS spectra on the chromatographic time scale is described. The emphasis is on design considerations and initial performance characterizations. This instrument (see Figure 1) utilizes TOF separation in both stages of mass analysis and a laser pulse to provide unit resolution selection of the precursor ion packet of interest, achieve high-efficiency photoinduced dissociation (PID), and yield a complete, unit-resolved product ion spectrum for each laser pulse.[1]

Photon-induced fragmentation by pulsed laser beam allows precursor ion selection by laser timing and provides efficient fragmentation in a manner that does not compromise the TOF analysis of the products. The high degree of photon–ion overlap at the interaction region, resulting from a focused ion packet and a focused laser pulse, results in the excitation of a large fraction of the selected ions and thus high fragmentation efficiencies. Because a useful normal or product spectrum can be obtained from each source extraction, it is practical to generate product spectra at the maximum laser repetition frequency (e.g., 200 Hz for pulsed excimer lasers). Since this rate of extraction is quite slow for TOF mass analysis, the generation of normal or primary spectra can be interspersed with product spectrum generation.

Several other researchers have designed tandem mass spectrometers which use photodissociation as the fragmentation method. Duncan et al. performed photodissociation in a single reflectron TOF mass spectrometer by intersecting a laser pulse and an ion packet at the turnaround point of the reflectron.[2] Schlag and co-workers also used a single reflectron TOF instrument to photodissociate benzene.[3] This was accomplished by focusing a laser pulse at the space focus plane outside the ion source and timing the laser pulse such that it intersected the isomass ion packet of choice. While demonstrating the practicality of PID in TOF instruments, these designs have not achieved our goal of unit mass resolution to *m/z* 1000 for both precursor and product ions.

Another related instrument is that of Cotter and Cornish.[4] They have constructed a tandem reflectron TOF mass spectrometer and used it to collect MS/MS data. Instead of using a laser for photodissociation in the fragmentation process, a gas pulse was used to perform collision-induced dissociation (CID) experiments.

EXPERIMENTAL SECTION

The instrument chamber has inner dimensions of 60 in. long × 11 in. wide × 9 in. tall with three removable access panels (~20

* Address reprint requests to Christie G. Enke, Department of Chemistry, 103 Clark Hall, University of New Mexico, Albuquerque, NM 87131. E-mail: enke@unm.edu.

† Current address: The Procter and Gamble Co., Sharon Woods Technical Center, 11450 Grooms Rd., Cincinnati, OH 45241.

(1) Seeterlin, M. A.; Vlasak, P. R.; Beussman, D. J.; McLane, R. D.; Enke, C. G. *J. Am. Soc. Mass Spectrom.* **1993**, *4*, 751–754.
(2) LaiHing, K.; Cheng, P. Y.; Taylor, T. G.; Willey, K. F.; Peschke, M.; Duncan, M. A. *Anal. Chem.* **1989**, *61*, 1458–1460.
(3) Boesl, U.; Weinkauf, R.; Walter, K.; Weickhardt, C.; Schlag, E. W. *Ber. Bunsenges. Phys. Chem.* **1990**, *94*, 1357–1362.
(4) Cornish, T.; Cotter, R. J. *Rapid Commun. Mass Spectrom.* **1992**, *6*, 242–248.

0003-2700/95/0367-3952$9.00/0

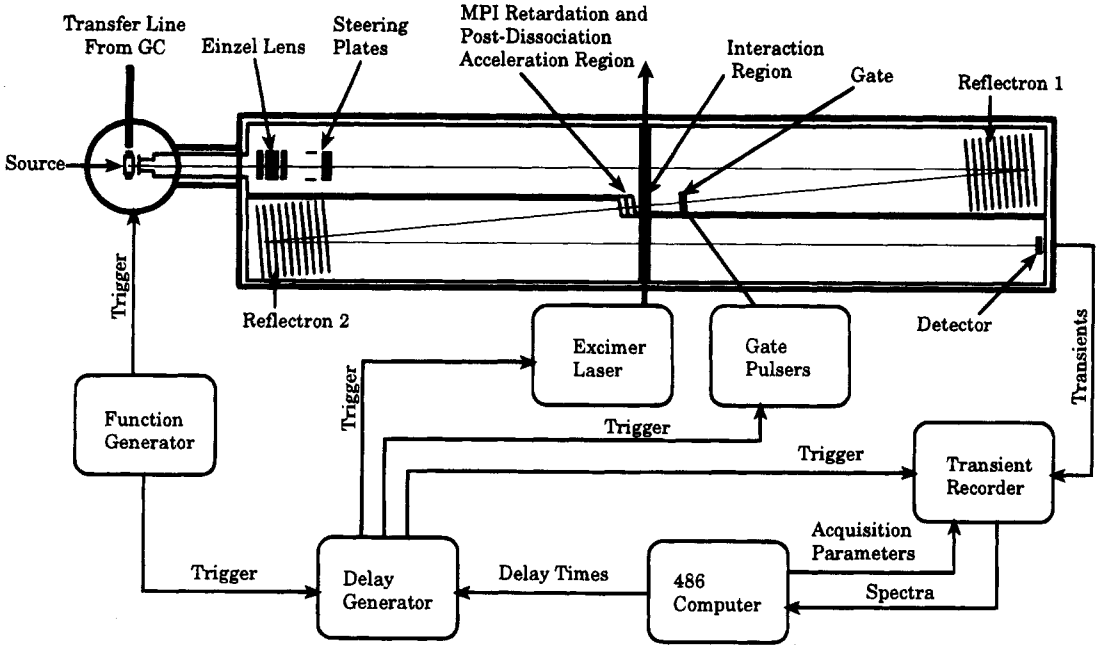

Figure 1. Schematic diagram of the tandem reflectron TOF mass spectrometer designed for photoinduced dissociation.

in. × 12 in.) in the top of the chamber to allow easy access to all areas of the instrument. The source housing is a six-way cross mounted on the end of the instrument chamber. A viewport is attached to the top of the source housing, and a heated GC transfer line (Finnigan, San Jose, CA) from a gas chromatograph (Model 5890, Hewlett-Packard, Palo Alto, CA) enters the source housing orthogonal to the ion flight path. The GC column terminates just inside the source region. The gaseous molecules resulting from continuous or injected sample introduction are allowed to spray into the source region, where electron impact ionization occurs continuously. One turbomolecular pump is mounted directly underneath the source, while a second is mounted on the underside of the chamber itself. The normal working pressure of the main chamber is between 3×10^{-7} and 6×10^{-7} Torr.

During ion extraction, a potential drop from the center of the source to the field-free region of 650 V is created. An Einzel lens is used to collimate the ion beam, while steering plates allow minor steering of the ion packets toward the first reflectron. High-voltage shields, constructed from stainless steel wire mesh (Newark Wire Cloth Co., Newark, NJ), line the inside of the instrument to create field-free flight paths. The shields for the first and second field-free regions are electrically isolated from the instrument chamber and from each other by $^3/_8$ in. ceramic spacers (NTT, Meadville, PA) attached to the mesh. The first reflectron consists of nine stainless steel electrodes and a stainless steel backplate. Each electrode is a 1 mm thick stainless steel ring with an outer diameter of 10.2 cm and an inner diameter of 6.3 cm.

The ion-deflection gate is constructed from two electrically isolated interleaved 0.003 in. diameter stainless steel wires. These wires are strung back and forth through alternate holes in two Vespel (E.I. du Pont de Nemours, Wilmington, DE) blocks, located on the top and bottom of the gate, such that they form a plane of 26 wire segments separated from each other by ~1 mm. The total dimensions of the wire gate are ~25 mm wide × 65 mm high.

Since the laser beam is of sufficient power to ablate metal, holes have been cut in the shield material to create an unimpeded path for the laser beam. To prevent field leakage through these holes, a tube has been constructed and placed through the holes such that the focused laser beam can pass through the tube without interacting with the shields or any other metal component inside the instrument. This tube is held at the potential of the first field-free region (−550 V). A second, shorter tube is slid over the first tube. This second tube just spans the width of the second field-free region and is at the same potential as the second field-free region shield (−2500 V). The two tubes are electrically isolated from each other by a thin sheet of Kapton (E.I. du Pont de Nemours, Wilmington, DE). Two 22 mm high × 34 mm wide holes have been cut out of opposite sides of the light tube where it intersects the ion flight path. In order to ensure that ion packets interact with photons only once along the flight path, the plane in which the z-shaped ion trajectory lies is tilted with respect to the laser beam path.

Three 5 cm × 5 cm grids, constructed from 88% ion transmission grid material (Buckbee-Mears, St. Paul, MN), are located just after the interaction region, with the first grid ~2 cm from the interaction region. The first grid is set at the field-free voltage of the first TOF stage (−550 V). The second grid has an applied potential ~20−30 V more positive than the first grid, which creates a retardation field to eliminate multiphoton ionization (MPI) products from reaching the detector. The potential applied to the third grid is that of the second field-free region. This creates an acceleration field after the interaction region. The grids which define the retardation and acceleration fields are separated by ~1 cm. The second reflectron in this instrument employs first two grids to provide a rapid deceleration region with a field strength of ~1565 V/cm and then a series of 10 gridless electrodes to produce a nonlinearly increasing field with a continuously decreasing field strength. This field shape was determined using a novel method for wide-energy-range reflectron design.[5] The electrodes are the same size and of the same material as those used in the first reflectron.

(5) Vlasak, P. R.; Beussman, D. J.; Ji, Q.; Enke, C. G. Manuscript in preparation.

Detection of the ions at the end of the second mass analyzer is achieved through the use of a dual 40 mm microchannel plate, chevron-type detector (modified Model TOF-2003, Galileo, Sturbridge, MA). The detector anode is connected to the input of the digital storage oscilloscope (described below) through a terminated 50Ω BNC cable. A second, removable detector with 25 mm microchannel plates has been constructed and mounted on a sliding carrier such that it can be placed anywhere along the rail beyond the interaction region. This allows detection and verification of ions after the interaction region components, ion focusing at the interaction region, and collection of crude spectra just beyond the interaction region in order to test the photodissociation process.

In the photodissociation experiments, a high-power Questek 2580 vβ excimer laser (Lambda-Physik, Acton, MA) is used to provide the necessary photons. This laser provides 150 mJ at 20 Hz using the ArF line (193 nm). The pulse width of the laser is ~15 ns. A cylindrical plano-convex fused silica (Dynasil 1100) lens (Newport, Irvine, CA) of 300 mm focal length is used to focus the laser beam to ~2 cm high × 1 mm wide at the interaction region inside the mass spectrometer. Two fused silica interferometer flats (Newport, Irvine, CA) are positioned on flanges mounted to the outside of the mass spectrometer in order to allow the photons to pass into the instrument and exit the other side, where they are collected in a beam dump device.

The electronics for all instrument components were designed and built in this lab, except for the high-voltage gate pulsers (Model GRX-1.5K-E, Directed Energy Inc., Fort Collins, CO). The timing sequence of the experiment is started by a square wave pulse from a function generator (Datapulse, Culver City, CA). This wave simultaneously triggers the pulser for the source backplate, a delay generator (Model 4222, LeCroy, Chestnut Ridge, NY), and a digital storage oscilloscope (Model 9450, LeCroy, Chestnut Ridge, NY). The source pulser then pulses the backplate from 0 to 200 V in order to extract the ions contained in the source volume. The four-channel delay generator provides timing, to within 1 ns, for the gate pulsers and the laser trigger. The delay generator and the digital oscilloscope are controlled through a general purpose interface bus connection (National Instruments, Austin TX) by a 486/33 computer (Zenith, St. Joseph, MI) running a control program written for LabWindows (National Instruments, Austin, TX).[6]

RESULTS AND DISCUSSION

Ion Source Considerations. Essential to the achievement of high sensitivity is the ability of the source to accumulate a significant fraction of the ions that are produced between the extraction pulses. This requires continuous ionization and some mechanism for retention of the ions produced. To this end, we have implemented a well-focused electron beam which produces a potential well between the backplate and the first grid.[7] This source design is similar to that of Wollnik and co-workers.[8] These sources have been shown to store ions between extraction pulses, thus increasing sensitivity.[9]

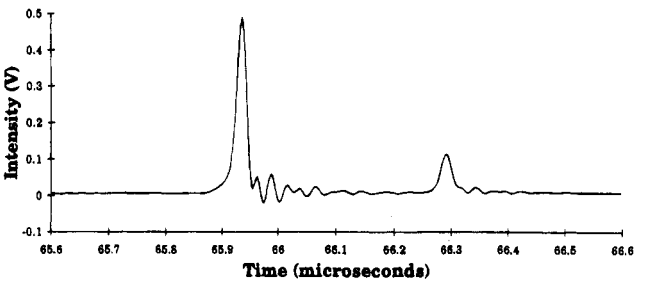

Figure 2. Normal EI spectrum of the molecular ion region of toluene (*m/z* 91–92), indicating a resolution of 1500 (fwhm) obtained at the interaction region (100 transients averaged). Peak width of 22 ns (fwhm) for *m/z* 91 (peak at 65.935 μs).

Precursor Ion Selection. Mamyrin et al. demonstrated a method of improving resolution using a reflectron.[10] Wollnik and Przewloka improved upon the Mamyrin reflectron TOF instrument by using grid-free reflectrons.[11] The grid-free devices do not suffer from ion transmission losses due to collisions with the grid material or loss of resolution associated with the field perturbations in the vicinity of the wire mesh;[12] they also serve to radially focus the ion packets. The first stage of mass analysis in the tandem TOF instrument was designed and constructed using a combination of the above technologies. As shown in Figure 2, a mass resolution of 1500 (fwhm) is obtained in the first TOF analyzer, as determined by placing a temporary detector at the interaction region.

To eliminate normal mass spectrum ions from the product spectrum, we have implemented an interleaved-comb ion deflection gate which can be quickly switched between ion deflection and ion transmission.[13] The ion gate is fashioned after a device first proposed by Loeb and studied theoretically by Lusk.[14] This device was further developed and used by Cravath,[15] as well as by Bradbury and Nielsen as an electron filter.[16] Later, Schlag et al.[17] adapted their design for use as an ion gate. When 250 and −250 V potentials, with respect to the field-free voltage, are applied to the alternate wires of the gate, the gate is "closed". In this state, each ion is deflected to the right or left. The gate is "open" when all the wires are set at the field-free voltage. A precursor ion packet is isolated by leaving the gate closed until the precursor ion packet is about to enter its field, at which time the gate is pulsed open until the precursor ion packet has passed through the space that the deflection field normally occupies. At this point, the gate is closed again, thereby deflecting all ions of higher *m/z* than the precursor ion packet and achieving precursor ion isolation.

The molecular ion region of bromobenzene (*m/z* 156–159) has been used to perform initial characterization of the ion gate. Figure 3A shows the normal molecular ion region of bromobenzene using a wide gate pulse, indicated by the gray box, to select

(6) McLane, R. D. Ph.D. Thesis, Michigan State University, East Lansing, MI, 1993.
(7) Studier, M. H. *Rev. Sci. Instrum.* **1963,** *34,* 1367–1370.
(8) Grix, R.; Grüner, U.; Li, G.; Stroh, H.; Wollnik, H. *Int. J. Mass Spectrom. Ion Phys.* **1989,** *93,* 323–330.
(9) Puzycki, M. A.; Gardner, B. D.; Allison, J.; Enke, C. G.; Grix, R.; Holland, J. F.; Yefchak, G. E. *Proceedings of the 39th ASMS Conference on Mass Spectrometry and Allied Topics*; Nashville, TN, May 19, 1991; p 156.
(10) Mamyrin, B. A.; Karataev, V. I.; Shmikk, D. V.; Zagulin, V. A. *Pis'ma Zh. Eksp. Teor. Fiz.* **1973,** *37,* 45–48.
(11) Wollnik, H.; Przewloka, M. *Int. J. Mass Spectrom. Ion Processes* **1990,** *96,* 267–274.
(12) Bergmann, T.; Martin, T. P.; Schaber, H. *Rev. Sci. Instrum.* **1989,** *60,* 347–349.
(13) Vlasak, P. R.; Beussman, D. J.; Davenport, M. R.; Enke, C. G. Manuscript in preparation.
(14) Loeb, L. B. *Basic Processes of Gaseous Electronics*; Univerisity of California Press: Berkeley, CA, 1961.
(15) Cravath, A. M. *Phys. Rev.* **1929,** *33,* 605–613.
(16) Bradbury, N. E.; Nielsen, R. A. *Phys. Rev.* **1936,** *49,* 388–393.
(17) Weinkauf, R.; Walter, K.; Weickhardt, C.; Boesl, U.; Schlag, E. W. *Z. Naturforsch.* **1989,** *44a,* 1219–1225.

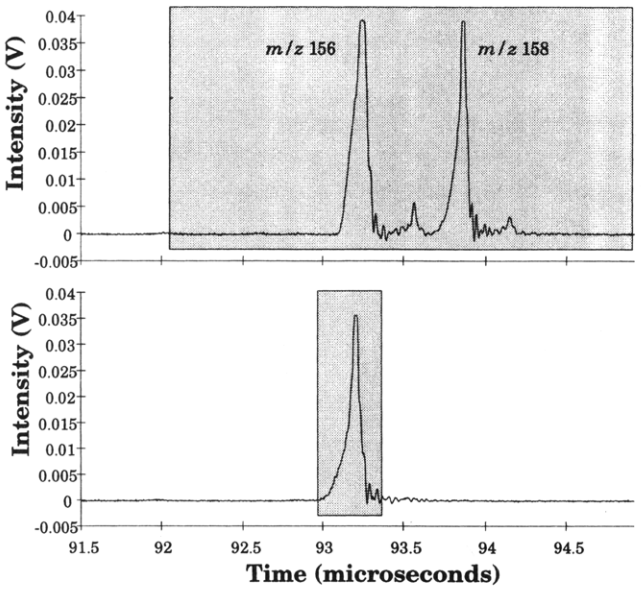

Figure 3. Spectra of the molecular ion region of bromobenzene, showing the ability to selectively gate an ion packet. The shaded regions indicate the gate "open" time window. Spectrum A shows a wide gate pulse, allowing *m/z* 153–161 to pass through. Spectrum B shows a narrow gate pulse used to selectively pass *m/z* 156 while deflecting all other *m/z* values.

the entire molecular ion region. In Figure 3B, the gate pulse is narrow and has been timed such that the *m/z* 156 ion packet has been selectively allowed to pass through the gate, while *m/z* 157–159 ions have been deflected away from the detector. The principal function of the gate in this instrument is to keep source ions of lower *m/z* value than the desired precursor ion packet out of the product spectrum. The actual precursor ion packet selection is determined by the coincidence of the laser photons and the precursor ion packet in the interaction region.

The focusing of the laser beam allows photons to interact with ions of only a single *m/z* value. Using the resolution for *m/z* 156 of bromobenzene obtained at the interaction region, the 1 mm spatial width of the laser beam, the 15 ns temporal width of the laser pulse, and the calculated ion velocity for each *m/z* value, the ability to selectively photodissociate a single *m/z* ion packet can be calculated. If the laser pulse is timed such that the photons at the midpoint of the laser pulse reach the interaction region at the same time as the midpoint of the ion packet, ~98% of the selected ion packet at *m/z* 156 is overlapped by the laser pulse, with no overlap or interference of neighboring *m/z* ion packets. At higher masses, the ability to selectively dissociate a single *m/z* ion packet is degraded due to the fact that the separation between adjacent *m/z* ion packets decreases, while the laser pulse dimensions remain the same. Also, since higher *m/z* ions have lower velocities than lower *m/z* ions, the higher *m/z* ions travel a shorter distance over the duration of the laser pulse, and thus a smaller fraction of a high *m/z* ion packet interacts with photons. At *m/z* 1000, the laser pulse interacts with 92% of the selected ion packet, but now 8% of the adjacent *m/z* ion packets also interact with the photons. The interference will be decreased if the mass resolution of the spectrum at the interaction region is increased, if the time between adjacent *m/z* ion packets is increased, or if the laser beam is focused to <1 mm. Critical to the achievement of this high level of precursor selectivity is the very small (~2 ns) jitter in the laser pulse timing.

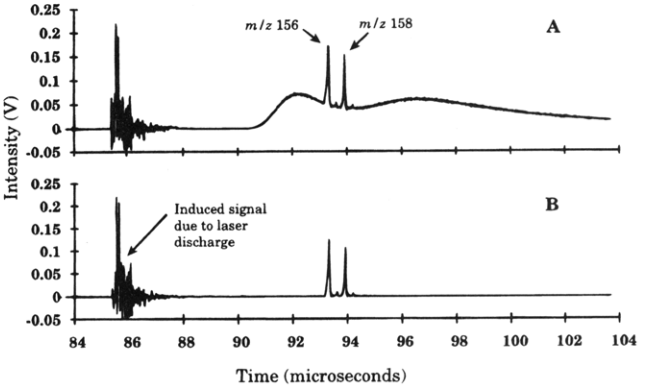

Figure 4. Spectra of the molecular ion region of bromobenzene (*m/z* 156–159) with laser discharge (indicated by sharp signal at ~86 μs) timed prior to ion arrival at the interaction region. Spectrum A shows the detection of MPI products causing interference with the EI spectrum. Spectrum B shows the use of the MPI retardation field, eliminating MPI interferences.

We have previously demonstrated experimentally the ability to selectively photodissociate a single *m/z* ion peak with this instrument.[1] Due to the linear relationship of flight time and square root of mass-to-charge ratio of ions in TOF mass spectrometry, the calibration of laser delay time is readily accomplished. The flight time to the temporary detector for a given *m/z* ion packet can be used to approximate the flight time of the ion packet to the interaction region in order to set an approximate laser delay time. Once the actual delay times required for ion–photon overlap for two *m/z* values have been determined, the flight time to the interaction region of any *m/z* ion packet can be calculated for the same instrument tune. This allows the laser delay time to easily be set so that the pulse interacts with any *m/z* ion packet of choice.

Pulsed Laser Photodissociation. The maximum fragmentation efficiency for photodissociation will be achieved at the maximum ion–photon overlap. The ion bunching nature of TOF mass spectrometry, as well as the fact that the ion packets are spatially focused to a narrow slice within the beam cross section at the interaction region, ensures a high ion density in this region. The photon beam is optically shaped to a beam 2 cm high × 1 mm wide to intercept the ion packet edge on. The very high photon and ion temporal and spatial overlap at the interaction region provides a maximum likelihood of photon and ion interaction. With this system, we have previously demonstrated efficiencies of 27%–79% for the photodissociation of various ions using 193 nm photons.[1]

The high photon flux also results in MPI of the background gas molecules present in our instrument. Unless discriminated against, these ions can then drift down the flight path and become accelerated by the postdissociation acceleration field. The resulting ion current due to these MPI products can convolute the mass spectrum. Figure 4A shows the resulting ion signal for the molecular ion region of bromobenzene with the detector placed ~20 cm past the interaction region. The sharp, noisy signal on the left is the induced signal in the detector due to the 30 kV discharge of the laser thyratron. The laser was timed such that the photons reached the interaction region just prior to molecular ions of bromobenzene; therefore, no PID products of bromobenzene ions were produced. The sharp peaks near the center of the spectrum are the undissociated molecular ions of bromobenzene (*m/z* 156 and 158). The broad peaks are due to the MPI

products reaching the detector and thus interfering with the normal mass spectrum of bromobenzene.

The MPI products in the interaction region have only the thermal kinetic energy that the background gas molecules have, while the PID products have a substantial fraction of the original precursor ion energy. To prevent the motion of the MPI products toward the analyzer, a slightly positive field (20–30 V) was introduced. Figure 4B shows a spectrum of the molecular ion region of bromobenzene, but with the addition of the MPI retardation field so that interference from the MPI products is eliminated. The laser discharge signal can again be seen, indicating that the laser has been fired and that ions are being created by MPI.

Product Ion Dispersion and Focusing. While the average velocity of the precursor ions of a particular *m/z* is mass-dependent, the velocity of the product ions formed by PID is approximately the same as that of their precursors. Some electric field gradient is required after the interaction region to separate the product ions in time. This is accomplished with the postdissociation acceleration field after the interaction region in order to impart mass-dependent velocities to the product ions. In order to maximize the product spectrum resolution, a temporal focusing system must compensate for the energy distribution of the isomass precursor ion packet that was focused at the interaction region (plus the additional kinetic energy distribution from the PID process), and it must do this for product ions whose average initial kinetic energies vary from a few percent to 100% of the average precursor ion energy.

All designs to date for achieving temporal focusing of mass-dispersed product ions involve the use of a reflectron. Scanning the reflectron voltage profile has been used to obtain focused product spectra,[17] but this solution is not consistent with our goal of achieving a complete product spectrum from each PID event. To avoid scanning the reflectron field strength, a curved-field reflectron has been implemented by Cornish and Cotter which serves both to time-disperse the product ions and to provide reasonable ion focus over the entire product ion *m/z* range.[18]

In our instrument, we have chosen to use an acceleration field of 1950 eV after the interaction region to provide mass-dependent product ion velocities. Since the product ions will retain some fraction of their initial 650 eV energy, the energy range of the accelerated product ions will be from 1950 to 2600 eV. This reduces the relative kinetic energy range of the product ions from nearly 100% to ~25% (defined as the energy range divided by the maximal energy).

Since the acceleration field provides the flight time dispersion of the various product ion masses, the second reflectron is used in its more traditional mode of focusing the different energies of the isomass product ions. Because the mean energy is different for each product ion *m/z* value, some field curvature in the reflectron is required to provide the correct field gradient at each turnaround point. The method by which we determined the optimum field shape and electrode voltages is described elsewhere.[5]

Figure 5 is the normal mass spectrum of toluene recorded at the final detector position. The resolution of this spectrum is ~1000, indicating that the resolution of a normal mass spectrum through the second reflectron is not severely degraded as

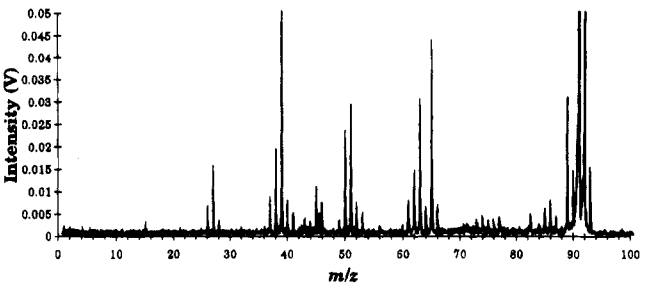

Figure 5. Normal EI spectrum of toluene (*m/z* 92), indicating a resolution of 1000 (fwhm) obtained at the final detector position (100 transients averaged). Peak intensities at *m/z* 91 and 92 are off-scale.

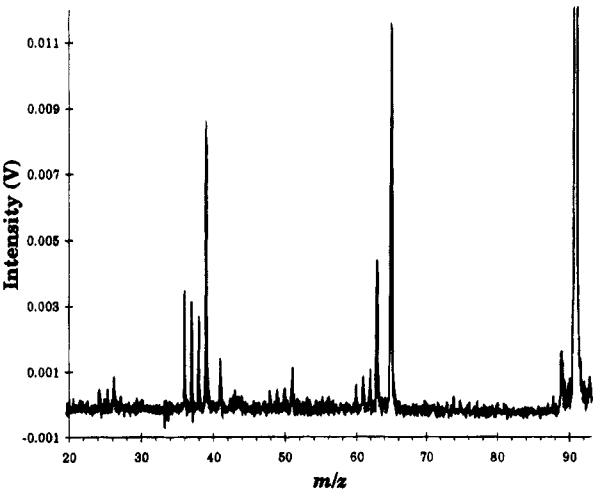

Figure 6. Product spectrum for *m/z* 91 of toluene, indicating a resolution of 300 (fwhm) obtained at the final detector position (200 transients averaged). Peaks due to the normal spectrum prior to *m/z* 91 have been eliminated by the ion gate.

compared to that from a spectrum recorded using the temporary detector placed in front of the second reflectron. Despite the longer path length, no increase in resolution is observed at the final detector. We believe this is primarily due to the increased number of grids that the ions must pass through, each of which degrades the resolution.[19] The resulting product spectrum from the photodissociation of *m/z* 91 from toluene is shown in Figure 6. The resolution of the spectrum is ~300 (m/Δm, fwhm). This spectrum represents a kinetic energy range of ~2035–2600 eV, or a 22% relative range. The resolution for the product spectrum is lower than that for a normal mass spectrum, but this is expected since in the normal spectrum isomass ion packets begin separating from one another just outside of the source, while the product isomass ion packets begin separating from each other only after the postdissociation acceleration. This leads to a time-compressed spectrum and therefore decreased resolution.

The mass axis of the product spectrum has been calibrated using the *m/z* values and flight times for the precursor ion and two product ions. Once a calibration has been determined, it can be used to calibrate product spectra from any precursor *m/z*, using the same instrument tune.

Overall Instrument Performance and Applications. Fragmentation efficiencies of up to 79% (for bromobenzene) have been obtained in our tandem TOF instrument. This represents a significant increase in the PID fragmentation efficiency compared

(18) Cornish, T. J.; Cotter, R. J. *Rapid Commun. Mass Spectrom.* **1993**, *7*, 1037–1040.

(19) Bergmann, T.; Martin, T. P.; Schaber, H. *Rev. Sci. Instrum.* **1989**, *60* (3), 347–349.

with earlier results obtained in an ion cyclotron mass spectrometer.[20] The efficiencies obtained in this instrument are comparable to those obtained using CID in a triple quadrupole mass spectrometer.[21]

Unit mass resolution to at least *m/z* 300 has been demonstrated for all components of the tandem TOF mass spectrometer. This is not a theoretical limit, but one that can be improved with further design refinements. Even the current resolution allows for both the selection of a single *m/z* ion packet for further fragmentation and the collection of resolved product spectra over the entire mass range. Since the instrument voltages do not need to be adjusted during an experiment, and since the photodissociation process is efficient, a full product spectrum of any *m/z* can be obtained for each ion extraction from the source.

In the analytical application of this instrument, a laser with a repetition rate of 200 Hz will be used, allowing up to 200 product spectra to be produced each second. With the incorporation of an integrating transient recorder like that developed at Michigan State University,[22] the continuous acquisition and storage of these spectra will be feasible. This will allow full MS/MS data to be collected on the time scale of a component elution from a gas chromatograph.

This instrument is also proving to be an ideal platform for studying the photodissociation of small ions. Laser wavelength and pulse energy can be varied to determine the effects on the fragmentation process. Also, the structural usefulness of the product ions can be determined and compared with those obtained using CID in other tandem mass spectrometers. This will allow for a determination of the analytical utility of photodissociation as a fragmentation method in MS/MS.

We intend also to increase the mass range of ions introduced into our tandem mass spectrometer by either replacing the EI source with a MALDI source[23] or using a novel ion trap source, being built by our group,[24] to attach an electrospray source to a TOF mass spectrometer. Since the energy imparted to an ion by a photon is independent of the ion's mass (unlike in CID, where the imparted energy decreases with increasing ion mass), PID may prove to be an advantageous fragmentation technique for high-mass ions. The implementation of the above sources will allow this to be investigated.

ACKNOWLEDGMENT

We gratefully acknowledge the National Institutes of Health for supporting this work (NIH GM 44077). H. Wollnik made several valuable suggestions during the initial design phase of this work. M. Rabb did much of the electronics system design and construction.

Received for review March 23, 1995. Accepted August 10, 1995.[⊗]

AC950288O

[⊗] Abstract published in *Advance ACS Abstracts*, September 15, 1995.

(20) Bowers, W. D.; Delbert, S.-S.; McIver, R. T., Jr. *Anal. Chem.* **1986**, *58*, 969–972.

(21) Yost, R. A.; Enke, C. G.; McGilvery, D. C.; Smith, D.; Morrison, J. D. *Int. J. Mass Spectrom. Ion Phys.* **1979**, *30*, 127–136.

(22) Holland, J. F.; Newcombe, B.; Tecklenburg, R. E., Jr.; Davenport, M.; Allison, J.; Watson, J. T.; Enke, C. G. *Rev. Sci. Instrum.* **1991**, *62*, 69–75.

(23) Gardner, B. D.; Vlasak, P. R.; Beussman, D. J.; Enke, C. G.; Watson, J. T. *Proceedings of the 42nd ASMS Conference on Mass Spectrometry and Allied Topics*; Chicago, IL, June 2, 1993; p 1037.

(24) Ji, Q.; Vlasak, P. R.; Holland, J. F.; Enke, C. G. *Proceedings of the 42nd ASMS Conference on Mass Spectrometry and Allied Topics*; Chicago, IL, June 2, 1993; p 1042.